

# Complex Relationship Between Changes in Oxygenation Status and Changes in $R_2^*$ : The Case of Insulin and NS-398, Two Inhibitors of Oxygen Consumption

Bénédicte F. Jordan,<sup>1,2</sup> Nathalie Crokart,<sup>1</sup> Christine Baudelet,<sup>1,2</sup> Greg. O Cron,<sup>1</sup> Réginald Ansiaux,<sup>1</sup> and Bernard Gallez<sup>1,2\*</sup>

Insulin and NS-398 have been reported to inhibit oxygen consumption in experimental tumor models, thereby increasing oxygenation and radiosensitization. The aim of this work was to use MRI to study changes in murine FSall tumor hemodynamics after administration of those oxygen consumption inhibitors. A multiple-echo gradient-echo (GRE) MRI sequence (4.7 T) was used to map changes in three factors: the GRE signal (at TE = 20 ms), the parameter  $S_0$  (theoretical signal at TE = 0 ms), and the relaxation rate  $R_2^*$ . Perfusion maps were obtained by dynamic contrast-enhanced (DCE) MRI. Insulin caused a significant decrease in the tumor blood oxygen level-dependent (BOLD) signal over time. factor This was likely the result of decreased blood flow, since both  $S_0$  and the percentage of perfused tumor decreased as well. Tumor  $R_2^*$  did not change significantly in response to the treatments, which is surprising considering that other non-MRI techniques (electron paramagnetic resonance (EPR) oximetry and fiber-optic probes) have shown that tumor oxygenation increases after treatment. This suggests that metabolic changes associated with vasoactive challenges may have an unpredictable influence on blood saturation and  $R_2^*$ . In conclusion, this study further emphasizes the fact that changes in BOLD signal and  $R_2^*$  in tumors do not depend uniquely on changes in oxygenation status. *Magn Reson Med* 56:637–643, 2006. © 2006 Wiley-Liss, Inc.

**Key words:** tumor; oxygenation; perfusion;  $T_2^*$ ; GRE-MRI; BOLD-MRI

Gradient-echo (GRE) images are sensitive to  $T_2^*$ , which is dependent on deoxyhemoglobin concentration. Hence, GRE images are dependent on blood oxygenation, producing the so-called blood oxygen level-dependent (BOLD) image contrast (1). BOLD is widely used to study functionality in the brain (functional MRI (fMRI)) (2). BOLD imaging has also recently become of particular interest in the field of tumor oxygenation, although this new application has generated many questions regarding interpretation of the BOLD signal in tumors (3–7). GRE images are also sensitive to flow (the in-flow effect) and therefore have the potential to monitor hemodynamic changes in two ways:

changes in the oxygenation of the blood, or changes in blood flow. Accordingly, this contrast is also designated as a flow and oxygenation-dependent (FLOOD) contrast, indicating that there are different underlying physiological changes compared to those of BOLD in the brain (6). Much work has been done to better understand the ways in which blood flow and oxygenation contribute to changes in image contrast in tumors (4,8,9). A positive correlation has usually been observed between the average increase in tumor  $T_2^*$  and increases in tumor oxygenation. However, this method has been demonstrated to be qualitative in nature and does not allow a true quantification of the oxygenation level (9). A potential application of the BOLD/FLOOD technique is to monitor the effectiveness of vascular modifiers on individual tumors and thereby provide a method for optimizing cancer treatments (6,7,10,11).

Tumor oxygenation is a critical determinant of tumor response to several treatment modalities, such as radiotherapy and chemotherapy (12). Hence, a number of tumor oxygenating treatments have been developed to improve therapeutic outcome. We previously investigated different treatments that led to nitric oxide-mediated modulations of tumor hemodynamic parameters and successfully radiosensitized experimental tumors. Among those treatments, insulin was of particular interest with regard to tumor radiosensitization (13). In one study (14) the effects of insulin were characterized in terms of tumor oxygenation, blood flow, and oxygen consumption rate.

In that study (14), local tumor oxygenation measurements were carried out using two independent techniques. One method employed electron paramagnetic resonance (EPR) oximetry and a fiber-optic device (OxyLite), and in the other technique blood flow inside the tumor was assessed using a laser Doppler system (OxyFlo) and dynamic contrast-enhanced (DCE)-MRI with a small molecular contrast agent (Gd-DTPA). Using this protocol, we obtained evidence that insulin increases the local pressure of oxygen of tumors (from 0–3 mm Hg to 8–11 mm Hg) as well as the tumor response to irradiation (increasing regrowth delay by a factor of 2.11). We found that the insulin-induced increase of tumor pressure of oxygen was not caused by an increase in the tumor blood flow, which was even decreased after insulin infusion, but rather was due to a decrease in the tumor cell oxygen consumption (in vivo insulin-treated tumor cells consumed oxygen three times more slowly than control cells). Theoretical modeling studies by Secomb et al. (14) showed that hypoxia was more efficiently reduced by a reduction in the oxygen consumption rate than by an increase in the oxygen sup-

<sup>1</sup>Laboratory of Biomedical Magnetic Resonance, Université Catholique de Louvain, Brussels, Belgium.

<sup>2</sup>Laboratory of Medicinal Chemistry and Radiopharmacy, Université Catholique de Louvain, Brussels, Belgium.

Grant sponsor: Belgian National Fund for Scientific Research; Grant number: 7.4503.02; Grant sponsor: Actions de Recherches Concertées-Communauté Française de Belgique; Grant number: ARC 04/09-317; Grant sponsor: Fonds Joseph Maisin.

\*Correspondence to: Prof. Bernard Gallez, Ph.D., CMFA/REMA Units, Avenue Mounier 73.40, B-1200 Brussels, Belgium. E-mail: Gallez@cmfa.ucl.ac.be

Received 12 July 2005; revised 7 April 2006; accepted 12 April 2006.

DOI 10.1002/mrm.20963

Published online 8 August 2006 in Wiley InterScience (www.interscience.wiley.com).

ply. NS-398, a nonsteroidal antiinflammatory drug (NSAID), was also shown to increase the radiosensitivity of tumors by increasing tumor oxygenation via the same mechanism as insulin (15).

The purpose of the present study was to use a multiecho GRE-MRI sequence to further characterize the effect of the two oxygen consumption inhibitors on BOLD signal intensity (SI, GRE signal at TE = 20 ms),  $S_0$  (theoretical GRE signal at TE = 0 ms), and  $R_2^*$  ( $= 1/T_2^*$ ). We also performed a DCE-MRI study using the rapid-clearance blood pool contrast agent P792 (Vistarem®) to determine how insulin and NS-398 affect  $K_{trans}$  and  $K_{ep}$  (parameters related to permeability), as well as  $V_p$  (plasma volume fraction) and the fraction of the tumor perfused by the contrast agent.

## MATERIALS AND METHODS

### Tumor Implantation and Treatments

Syngeneic FSaII fibrosarcomas were inoculated into the hind leg muscle of male C3H/HeOJ]co mice. The mice were imaged when the tumors were  $9 \pm 1$  mm in diameter (10 days later). For imaging, the mice were anesthetized with 1.4–2.0% isoflurane carried in 21% oxygen in a continuous flow (1.5 l/hr). Warm air was flushed into the magnet in order to maintain normothermia. Insulin (Actrapid HM; Novo Nordisk, Bagsvaerd, Denmark) was infused via a tail vein catheter at a rate of 16 mU/kg/min for 25 min. Control mice were infused with a 0.9% NaCl solution (saline) at the same rate for the same length of time as for insulin. NS-398, [N-[2(Cyclohexyloxy)4-nitrophenyl-methanesulfonamide] (2 mg/ml in DMSO; Alexis Biochemicals) was administered by IP injection at a dose of 10 mg/kg.

### Imaging

MRI was performed with a 4.7 T (200 MHz, 1H), 40-cm inner diameter horizontal bore system (Bruker Biospec, Ettlingen, Germany). The mice were positioned in a 70-mm inner diameter birdcage radiofrequency coil.  $T_2$ -weighted anatomical images were acquired using a fast spin echo sequence (TR = 4 s, effective TE = 50 ms).

All MRI data were processed offline with a program written in house using IDL™ (Interactive Data Language; RSI, Boulder, CO, USA) development software.

### DCE MRI

With the use of DCE-MRI, it is possible to generate parametric maps that reflect the plasma volume fraction, the permeability, and the rate of efflux, as described previously (16). Imaging was commenced 35 min after the end of the insulin ( $N = 5$ ) or saline ( $N = 5$ ) treatments (i.e., 1 hr after the start of the treatments). NS-398 ( $N = 5$ ) was administered in a single injection 30 min before imaging. Prior to DCE imaging, proton density-weighted (PDw) images were acquired with the following parameters: TR = 8 s, TE = 4.9 ms, number of averages (NA) = 2, flip angle = 90°, FOV = 4 cm, slice thickness = 1.6 mm, matrix =  $64 \times 64$ , two slices (one slice through the kidneys and one through the center of the tumor). For DCE  $T_1$ -weighted imaging, a gradient-recalled echo sequence was used with

the following parameters: TR = 40 ms, TE = 4.9 ms, NA = 1, flip angle = 90°, geometry parameters = same as for the PDw sequence, scan time per image = 2.56 s. The contrast agent P792 (Vistarem®; Laboratoire Guerbet, Aulnay sous Bois, France), a rapid-clearance blood pool agent, was injected intravenously as a bolus (injection duration = 2 s) at a dose of 0.042 mmol Gd/kg (50  $\mu$ l/40 g mouse) (17). The DCE imaging protocol was as follows: 12 baseline images were acquired, and then P792 was injected and the enhancement kinetics were continuously monitored for 8 min (200 total scans) in order to track the fast washing kinetics. Immediately after this, a slower DCE data set was acquired to monitor the washout of the contrast agent. For this second set, 60 scans were acquired at a temporal resolution of 60 s (NA = 24, 1 hr total).

For postprocessing, tumor voxels that showed no signal enhancement, a linear increase of SI, or atypical signal enhancement curves were excluded by means of a power spectrum analysis and cluster analysis (18,19). Contrast agent concentration as a function of time after P792 injection ( $C(t)$ ) was estimated using the following equation:

$$C(t) = \left( \frac{1}{TR \cdot r_1} \right) \ln \left[ \left( 1 - \frac{S_{O_{T1w}}}{S_{O_{PD}}} \right) / \left( 1 - \frac{S(t)}{S_{O_{PD}}} \right) \right] \quad [1]$$

where TR is the repetition time of the PDw image, and  $r_1$  is the relaxivity of the contrast agent (9 mM<sup>-1</sup>s<sup>-1</sup>). The tracer concentration changes were fitted to a two-compartment pharmacokinetic model (20) using an arterial input function derived from kidney data as described previously (16,20). Pixel-by-pixel values for  $K_{trans}$  (influx volume transfer constant, from plasma into the interstitial space, units of min<sup>-1</sup>),  $V_p$  (blood plasma volume per unit volume of tissue, unitless), and  $K_{ep}$  (fractional rate of efflux from the interstitial space back to blood, units of min<sup>-1</sup>) in tumor were derived from this model. Statistical significance for  $V_p$  or  $K_{trans}$  identified the percentage of “perfused” tumor pixels (i.e., pixels to which the contrast agent P792 had access).

### $T_2^*$ GRE MRI

A multiecho GRE sequence was used to calculate the GRE SI,  $R_2^*$ , and  $S_0$ , on a pixel-by-pixel basis in each tumor. The sequence parameters were TR = 200 ms, six echoes with an echo spacing of 5 ms (TE = 5, 10, 15, 20, 25, 30 ms), spectral width = 25 kHz, flip angle = 45°, matrix size =  $64 \times 64$ , FOV = 4 cm, slice thickness = 1.6 mm, NA = 10, total acquisition time = 128 s. These conditions enabled us to sample the free induction decay (FID) properly, since the basal tumor  $T_2^*$  was  $29.7 \pm 8.5$  ms (mean  $\pm$  SD). MRI data were acquired continuously for 1 hr 45 min (50 repetitions), with either insulin ( $N = 6$ ) or saline ( $N = 6$ ) infused between repetitions 5 and 17, or NS-398 ( $N = 5$ ) administered at repetition 5. For each repetition, a mono-exponential function was used to fit the GRE signal as a function of TE. Voxels with a bad fitting were set to zero to avoid aberrant values (outside the 0–200 ms interval’s limits for  $T_2^*$ ). The number of failed pixels was fairly low and was shown to be constant over time (5%  $\pm$  2%). The GRE SI was taken to be the GRE signal at TE = 20 ms. The parameters  $R_2^*$  ( $= 1/T_2^*$ ) and  $S_0$  (theoretical GRE signal at

TE = 0 ms) were determined as fit parameters in the monoexponential function. The fitting was performed only on the odd echoes, although the results were similar while using the even echoes. The relative change in GRE SI (%ΔSI) was calculated as a function of time as  $100 \times SI_{\text{post}}/SI_{\text{pre}}$ , where  $SI_{\text{post}}$  is the GRE signal as a function of time after the infusion of insulin or saline, and  $SI_{\text{pre}}$  is the average GRE signal before infusion of insulin or saline. Relative changes in  $S_0$  were expressed similarly ( $100 \times S_{0\text{post}}/S_{0\text{pre}}$ ). We verified the quality of the shimming for each study by measuring the linewidth of the water peak.

The changes in  $R_2^*$  ( $\Delta R_2^*$ ) and %ΔSI are parameters that are proportional to the change in deoxyhemoglobin content. These two parameters are independent of native tissue  $R_2^*$ , unlike  $\Delta T_2^*$  and the absolute change in SI (16). Therefore, treated and control groups were compared in terms of %ΔSI,  $\Delta R_2^*$ , and the relative change in  $S_0$ .

### Statistical Analysis

The results are presented as the means  $\pm$  SE. Comparisons between groups were analyzed by *t*-test (two-sided) or one-way analysis of variance (ANOVA) with Dunnett's post-hoc test.

## RESULTS

### Effects of Insulin and NS-398 on Tumor Perfusion

Figure 1 shows that insulin infusion had no effect on the average tumor  $K_{\text{trans}}$ ,  $K_{\text{ep}}$ , or  $V_p$  compared to controls. However, the fraction of perfused tumor pixels for the insulin-treated group was significantly lower than that of controls ( $56.3\% \pm 7.2\%$  vs.  $71.2\% \pm 4.5\%$ , respectively,  $P < 0.05$ ), indicating that fewer tumor regions are perfused after insulin. An important decrease in perfused pixels was also observed 30 min after NS-398 injection (decrease of  $50.5\% \pm 12.3\%$ ,  $P < 0.01$ ; Fig. 2), showing that the perfusion is significantly reduced by NS-398. The value of  $V_p$  (plasmatic volume fraction) was unchanged, and the permeability ( $K_{\text{trans}}$  and  $K_{\text{ep}}$ ) was significantly decreased in this case (15).

### Effect of Insulin and NS-398 on the GRE SI and $\Delta R_2^*$

Figure 3 shows that insulin infusion led to a significant decrease in %SI over time ( $7.5\% \pm 0.6\%$ ). The %SI decreased continuously from the 20-min time point ( $P < 0.05$ ) until at least 60 min after the end of the insulin infusion (end of measurement). A similar pattern was observed for the relative change in  $S_0$ , with a maximum decrease of  $4.6\% \pm 1.0\%$ .  $\Delta R_2^*$  was not significantly affected at any of the time points. For control mice, no significant changes were observed over time for any of the parameters (SEM = 0.7%, 0.9%, and 0.9% for  $\Delta R_2^*$ , BOLD, and  $S_0$ , respectively). A cluster analysis of the BOLD (GRE) signal was performed in order to take into account the tumor heterogeneity. In the insulin-treated group, about 40% of the tumor pixels remained stable, another 40% significantly decreased, and the remaining 20% increased, resulting in an overall decrease in the relative GRE SI. In the control group, the proportion of increasing and de-

creasing pixels was similar (30% each), resulting in a lack of change in the average relative GRE SI.

Similar results were observed using NS-398. %SI decreased continuously after NS-398 injection ( $P < 0.01$ ) until 1 hr after administration (end of measurement), a similar decrease was observed for  $S_0$ , and  $\Delta R_2^*$  was not significantly affected at any of the time points.

## DISCUSSION

We previously showed that insulin induces dramatic hemodynamic changes in experimental tumors (13). These changes are mostly characterized by an important increase in oxygenation and a slight decrease in blood flow. The improvement in tumor oxygenation was shown to be related to a decrease in oxygen consumption by tumor cells, rather than to an increase in oxygen supply (blood flow). The decrease in perfusion is likely due to a vascular steal effect with a redistribution of the blood flow that feeds the tumor and the muscle. More recently, we observed that NS-398, an antiinflammatory agent, induced a similar effect in the same tumor model (15).

Since  $pO_2$  and blood flow are altered in opposite ways after insulin and NS-398 administration, and since the BOLD signal is known to have multiple components (dependent on flow and oxygenation), we believed it was particularly relevant to study the evolution of the BOLD (GRE) signal over time after treatment.

Accordingly, in this study we characterized the hemodynamic changes induced by insulin and NS-398 with multiple GRE-MRI and DCE-MRI. Our group previously applied these techniques to study physiological noise as a marker of tumor acute hypoxia or the effect of anesthetics and different vasoactive agents, such as carbogen, nicotinamide, and pentoxifylline (7).

In this study we observed a significant decrease in the relative GRE SI over time when tumors were treated with insulin and NS-398. This SI was dependent on  $S_0$  (which was observed to decrease with time) and  $R_2^*$  (which did not change). Therefore, the decrease in the relative GRE signal is likely the result of a decrease in tumor blood flow, since both  $S_0$  (which is sensitive to  $T_1$  and therefore inflow effects) and the fraction of perfused pixels decreased. This result is confirmed by the typical pattern observed in parametric maps shown in Fig. 4. In this figure we can observe that the decrease in  $\Delta SI$  is correlated more to the decrease in  $\Delta S_0$  than to the  $\Delta R_2^*$ , which is globally unchanged for the entire tumor (i.e., the same amount of increasing and decreasing voxels).

It is somewhat surprising to observe an increase in tumor oxygenation along with a decrease in blood flow. In addition to the fact that the increase in  $pO_2$  observed here is the result of a decrease in oxygen consumption rate by the tumor cells (and thus is independent of any flow effect), it is important to note that blood flow is sampled on a pixel-by-pixel analysis, while  $pO_2$  is sampled on more than one pixel at a time (even though it is still a "local" measurement). The measured  $pO_2$  is thus an "averaged" value of different pixels that might individually show different patterns in terms of blood flow (e.g., a lack of change, slight decrease, or complete cessation of flow).

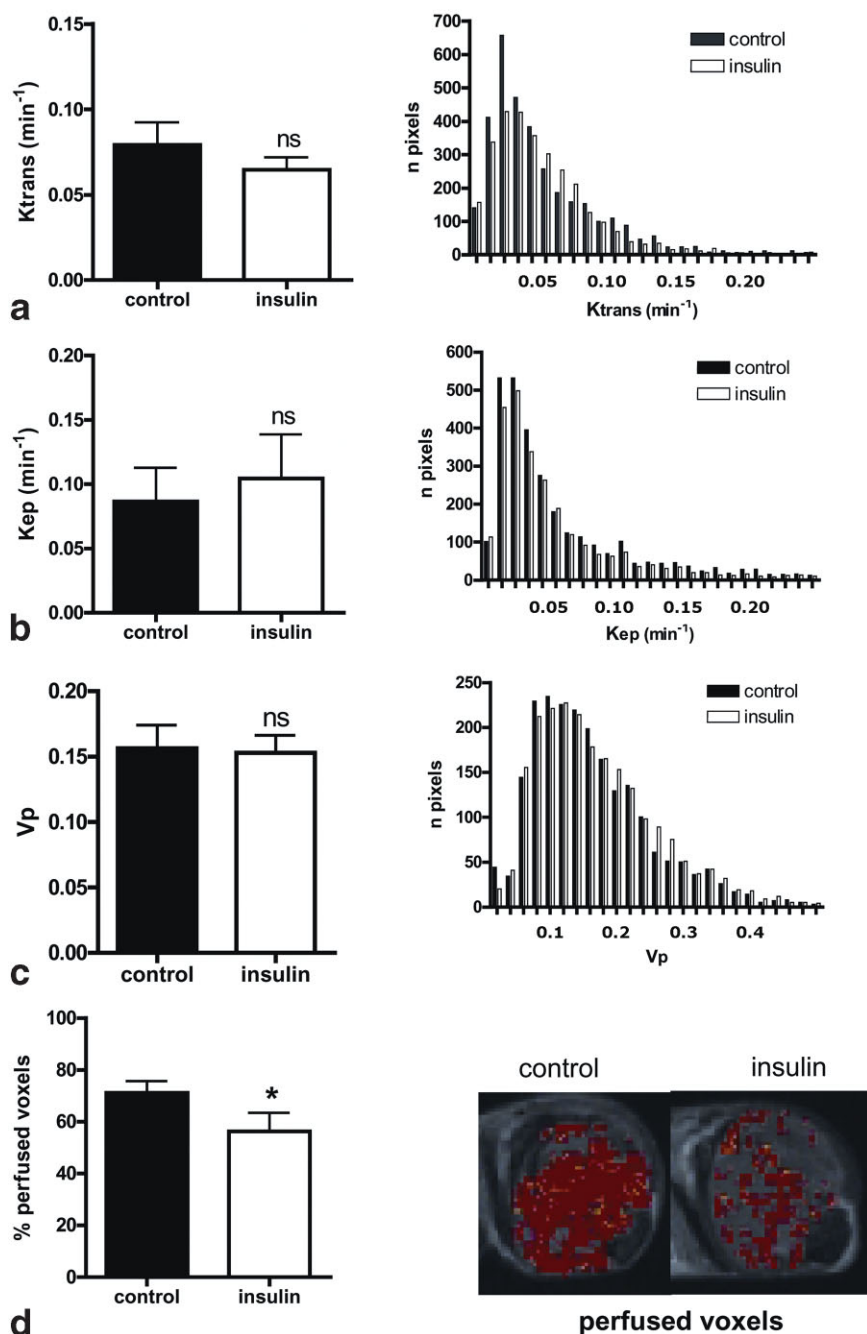


FIG. 1. Hemodynamic parameters measured in FSaII tumors after insulin treatment using DCE-MRI. The results are presented in cumulative relative frequency (left) and frequency distribution (right). **a:**  $K_{trans}$ , the influx volume transfer constant from plasma into the interstitial space. **b:**  $K_{ep}$ , the fractional rate of efflux from the interstitial space back to the plasma. **c:**  $V_p$ , the plasma volume fraction. **d:** The fraction of perfused tumor voxels, and a typical image of perfused voxels in a tumor. Values are the mean of five mice. Open columns, insulin-treated tumors; filled bars, control tumors. Note that  $K_{trans}$ ,  $K_{ep}$ , and  $V_p$  were unchanged after insulin treatment, while the fraction of perfused tumor voxels was significantly decreased.

$R_2^*$  did not change significantly in insulin-treated mice. The mean change in  $R_2^*$  is therefore not correlated with the changes in  $pO_2$  measured with EPR oximetry or with the fiber-optic probes (OxyLite™, which are based on the oxygen-quenched lifetime of a luminescent ruthenium dye), measured on the same FSaII tumor model. In the latter experiments, tumor  $pO_2$  was observed to rise up to ~10 mmHg (from a baseline of ~3 mmHg), which was the result of a threefold decrease in oxygen consumption rate by the tumor cells.

To help explain the discrepancy between these changes in  $pO_2$  and the lack of change in  $R_2^*$  observed in the current study, we note that EPR and OxyLite™ provide extracellular measurements, whereas  $\Delta R_2^*$  results from the intravas-

cular compartment only. An additional issue with OxyLite™ and EPR spectroscopy is that they report on local tissue  $pO_2$ , whereas BOLD MRI provides an index over the whole tumor. The localized EPR measurements correspond to an average of  $pO_2$  values in a volume of 10 mm<sup>3</sup> Hg (21). This technique has been extensively validated in our laboratory and was used to identify numerous radiosensitizing compounds (21). Moreover, the reproducibility of the results obtained with both techniques (EPR and fiber-optic probes), as well as in mice, suggests that the effect should not be completely heterogeneous inside the tumor. It is also unlikely that our paramagnetic or fiber-optic probes would have been systematically implanted in a region with a particular behavior in  $R_2^*$ , especially since

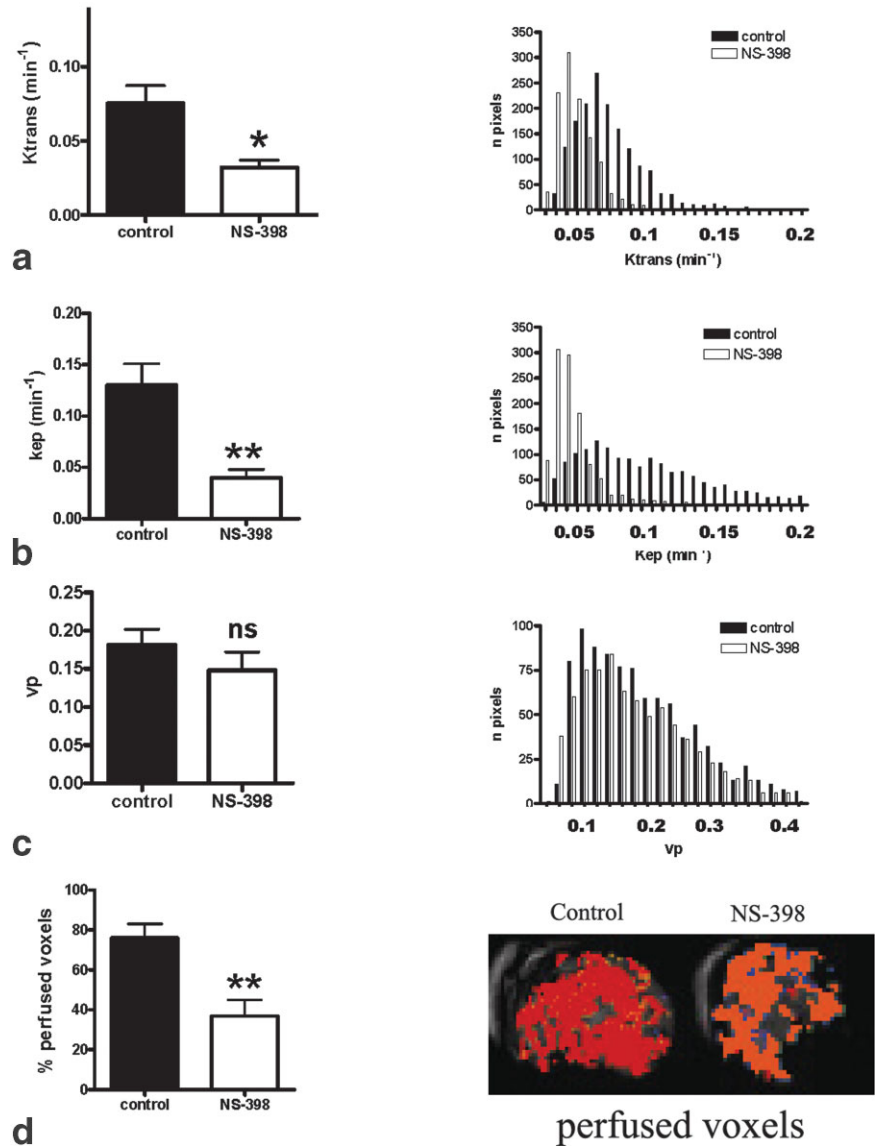


FIG. 2. Hemodynamic parameters measured in FSall tumors after NS-398 treatment using DCE-MRI. The results are presented in cumulative relative frequency (left) and frequency distribution (right). **a:**  $K_{trans}$ , the influx volume transfer constant from plasma into the interstitial space. **b:**  $K_{ep}$ , the fractional rate of efflux from the interstitial space back to the plasma. **c:**  $V_p$ , the plasma volume fraction. **d:** The fraction of perfused tumor voxels, and a typical image of perfused voxels in a tumor. Values are the mean of five mice. Open columns, NS-398-treated tumors; filled bars, control tumors. Note that  $V_p$  was unchanged and the permeability ( $K_{trans}$ ,  $K_{ep}$ ) was significantly decreased. The fraction of perfused tumor voxels was also significantly decreased.

pixels with changes in  $R_2^*$  were randomly distributed rather than grouped in a given region. EPR imaging using soluble materials that are able to diffuse into the area of interest could potentially extend the application of this technique to 3D measurements of oxygen tension, albeit with diminished sensitivity (max 5 mmHg accuracy) (19).

Other factors may also explain this discrepancy. A previous study noted that changes in  $R_2^*$  are not always indicative of changes in  $pO_2$  (7). Concomitant changes in blood volume, blood pH, or metabolic status can lead to smaller than expected or even negative changes in  $R_2^*$ . The blood volume is probably not involved in this case, since the DCE study did not show any change in  $V_p$ . However, the metabolic status of the tumor was previously shown to be profoundly affected after insulin infusion (13). An increase of the anaerobic glycolytic pathway activity resulting in an increase in the tumor lactate content was shown. These results confirm that metabolic changes associated with vasoactive challenges can have an unpredictable influence on blood saturation and  $R_2^*$ . In this field, it would

be particularly interesting to study other modifiers of oxygen consumption by tumor cells with GRE imaging, such as acute hyperglycemia (22) and meta-iodobenzylguanidine (MIBG) (23).

Finally, it is also important to note that we did not take into account the importance of spectrally inhomogeneous changes in the water resonance in this study. Small BOLD contrast changes can be caused by small deviations from the Lorentzian lineshape, which are difficult to detect by fitting the spectra. Interpretation of the results would benefit from high spectral and spatial resolution (HISS) imaging, which has been shown to detect these changes more accurately than conventional GRE imaging (24).

In conclusion, this study further emphasizes the fact that the BOLD contrast and  $\Delta R_2^*$  in tumors are not uniquely interpretable in terms of tumor oxygenation status. In the case of insulin, which inhibits the oxygen consumption rate by tumor cells, it is clear that a lack of change in  $R_2^*$ , or even a decrease in the relative GRE SI, does not necessarily mean that tumor oxygenation has not improved. Tumor  $T_2^*$  w GRE

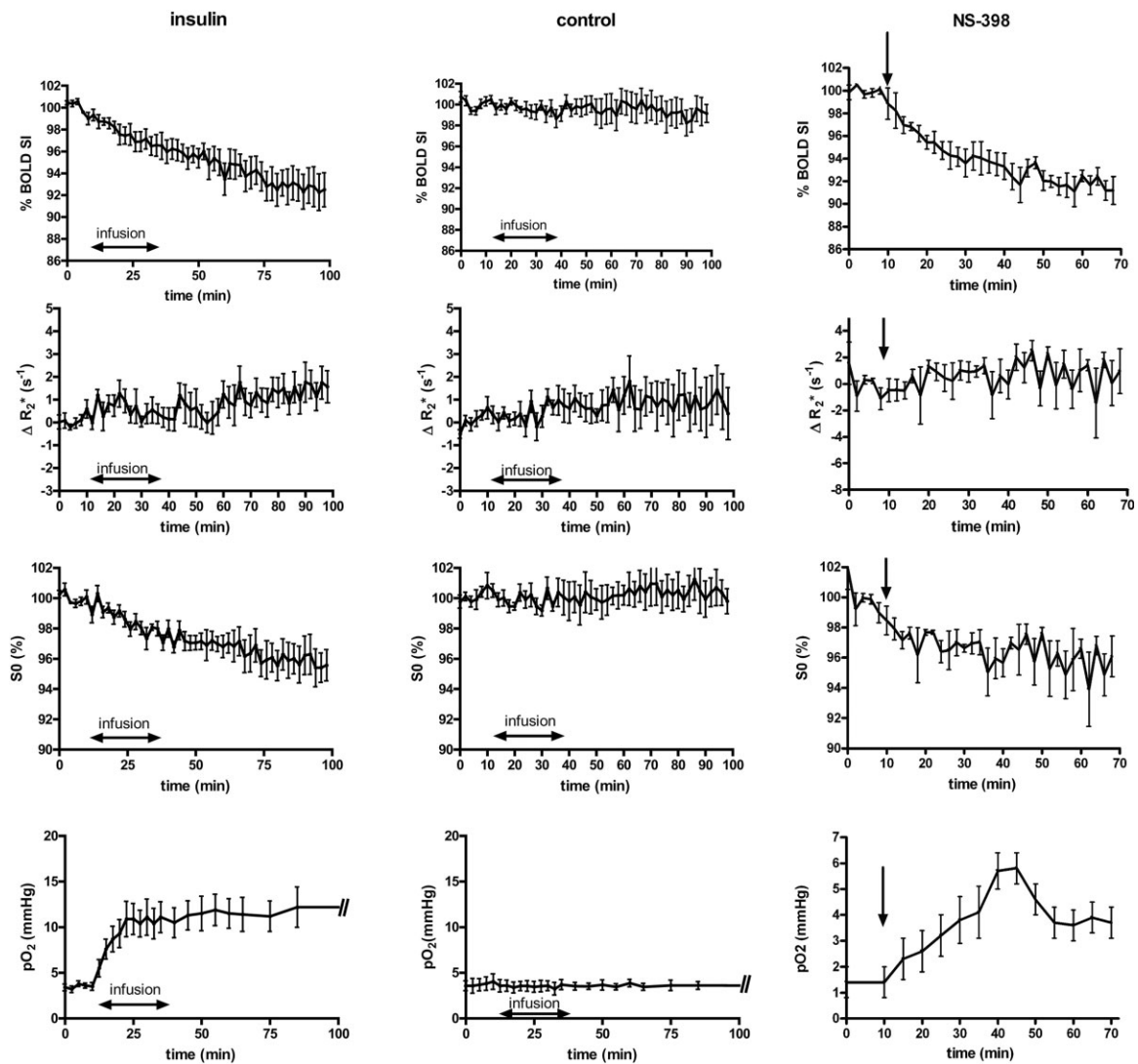


FIG. 3. Effects of insulin and NS-398 treatment on the hemodynamic parameters using a multiple-echo GRE sequence. The evolution over time of three factors (the GRE signal (top row), the variation in relaxation rate  $R_2^*$  (second row), and the parameter  $S_0$  (theoretical signal at TE = 0 ms, third row) is shown. Left, insulin-treated tumors; middle, control tumors; right, NS-398-treated tumors. Values are the mean of six mice for insulin and control, and five mice for NS-398. The bottom row shows the evolution of  $pO_2$  as a function of time measured by EPR oximetry (adapted from Refs. 14 and 16).  $pO_2$  values are the mean of five mice for insulin and control, and seven mice for NS-398. Note that the BOLD SI and  $S_0$  decreased with time, while the  $R_2^*$  was stable. Note also that the  $R_2^*$  does not correlate with the evolution of the  $pO_2$ .

MRI results should therefore be interpreted with caution. One may have to take other hemodynamic or metabolic changes into account while trying to interpret BOLD results.

Independent measurements of factors such as oxygen and blood flow should therefore be performed in order to better characterize tumor hemodynamic changes.

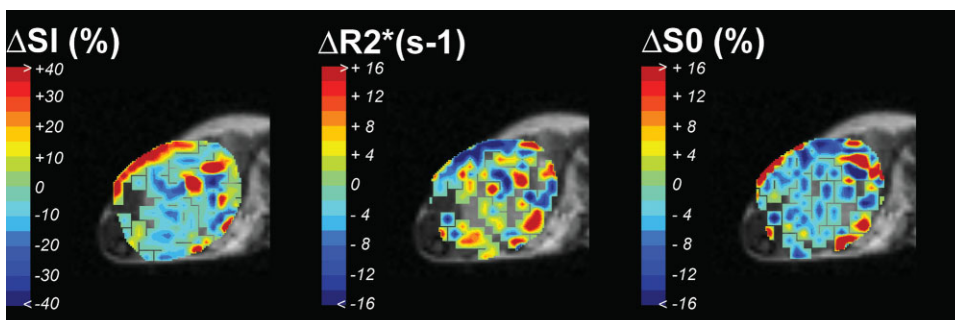


FIG. 4. Typical parametric maps of changes in GRE SI (%) (left),  $R_2^*$  ( $s^{-1}$ ) (middle), and  $S_0$  (%) (right) after an insulin challenge. We can observe that the decrease in  $\Delta SI$  correlates more to the decrease in  $\Delta S_0$  than to  $\Delta R_2^*$ , which is globally unchanged for the entire tumor (i.e., the same amount of increasing and decreasing voxels).

## ACKNOWLEDGMENTS

B.F. Jordan and C. Baudelet are postdoctoral researchers supported by the Belgian National Fund for Scientific Research. The authors thank Guerbet Laboratories (Roissy, France) for providing the P792.

## REFERENCES

- Ogawa S, Lee TM, Nayak AS, Glynn P. Oxygenation-sensitive contrast in magnetic resonance image of rodent brain at high magnetic fields. *Magn Reson Med* 1990;14:68–78.
- Hennig J, Speck O, Koch MA, Weiller C. Functional magnetic resonance imaging: a review of methodological aspects and clinical applications. *J Magn Reson Imaging* 2003;18:1–15.
- Griffiths JR, Taylor NJ, Howe FA, Saunders MI, Robinson SP, Hoskin PJ, Powell ME, Thoumine M, Caine LA, Baddeley H. The response of human tumors to carbogen breathing, monitored by gradient-recalled echo magnetic resonance imaging. *Int J Radiat Oncol Biol Physiol* 1997;39:697–701.
- Howe FA, Robinson SP, Rodrigues LM, Stubbs M, Griffiths JR. Issues in GRE & SE magnetic resonance imaging to probe tumor oxygenation. *Adv Exp Med Biol* 2003;530:441–448.
- Karczmar GS, River JN, Li J, Vijayakumar S, Goldman Z, Lewis MZ. Effects of hyperoxia on T<sub>2</sub>\* and resonance frequency weighted magnetic resonance images of rodent tumours. *NMR Biomed* 1994;7:3–11.
- Robinson SP, Collingridge DR, Howe FA, Rodrigues LM, Chaplin DJ, Griffiths JR. Tumour response to hypercapnia and hyperoxia monitored by FLOOD magnetic resonance imaging. *NMR Biomed* 1999;12:98–106.
- Baudelet C, Gallez B. Current issues in the utility of blood oxygen level dependent MRI for the assessment of modulations in tumor oxygenation. *Curr Med Imaging Rev* 2005;1:229–249.
- Al Hallaq HA, River JN, Zamora M, Oikawa H, Karczmar GS. Correlation of magnetic resonance and oxygen microelectrode measurements of carbogen-induced changes in tumor oxygenation. *Int J Radiat Oncol Biol Physiol* 1998;41:151–159.
- Baudelet C, Gallez B. How does blood oxygen level-dependent (BOLD) contrast correlate with oxygen partial pressure (pO<sub>2</sub>) inside tumors? *Magn Reson Med* 2002;48:980–986.
- Fan X, River JN, Zamora M, Al Hallaq HA, Karczmar GS. Effect of carbogen on tumor oxygenation: combined fluorine-19 and proton MRI measurements. *Int J Radiat Oncol Biol Physiol*. 2002;54:1202–1209.
- Rodrigues LM, Howe FA, Griffiths JR, Robinson SP. Tumor R<sub>2</sub>\* is a prognostic indicator of acute radiotherapeutic response in rodent tumors. *J Magn Reson Imaging* 2004;19:482–488.
- Vaupel P, Kallinowski F, Okunieff P. Blood flow, oxygen and nutrient supply, and metabolic microenvironment of human tumors: a review. *Cancer Res* 1989;49:6449–6465.
- Jordan BF, Gregoire V, Demeure RJ, Sonveaux P, Feron O, O'Hara J, Vanhulle VP, Delzenne N, Gallez B. Insulin increases the sensitivity of tumors to irradiation: involvement of an increase in tumor oxygenation mediated by a nitric oxide-dependent decrease of the tumor cells oxygen consumption. *Cancer Res* 2002;62:3555–3561.
- Secomb TW, Hsu R, Ong ET, Gross JF, Dewhirst MW. Analysis of the effects of oxygen supply and demand on hypoxic fraction in tumors. *Acta Oncol* 1995;34:313–316.
- Crocart N, Radermacher K, Jordan BF, Baudelet C, Cron GO, Gregoire V, Beghein N, Bouzin C, Feron O, Gallez B. Tumor radiosensitization by antiinflammatory drugs: evidence for a new mechanism involving the oxygen effect. *Cancer Res* 2005;65:7911–7916.
- Baudelet C, Ansiaux R, Jordan BF, Havaux X, Macq B, Gallez B. Physiological noise in murine solid tumours using T<sub>2</sub>\*-weighted gradient-echo imaging: a marker of tumour acute hypoxia? *Phys Med Biol* 2004;49:3389–3411.
- Fan X, Medved M, River JN, Zamora M, Corot C, Robert P, Bourrinet P, Lipton M, Culp RM, Karczmar GS. New model for analysis of dynamic contrast-enhanced MRI data distinguishes metastatic from nonmetastatic transplanted rodent prostate tumors. *Magn Reson Med* 2004;51:487–494.
- Baudelet C, Gallez B. Cluster analysis of BOLD fMRI time series in tumors to study the heterogeneity of hemodynamic response to treatment. *Magn Reson Med* 2003;49:985–990.
- Gallez B, Baudelet C, Jordan BF. Assessment of tumor oxygenation by electron paramagnetic resonance: principles and applications. *NMR Biomed* 2004;17:240–262.
- Tofts PS, Brix G, Buckley DL, Evelhoch JL, Henderson E, Knopp MV, Larsson HB, Lee TY, Mayr NA, Parker GJ, Port RE, Taylor J, Weisskoff RM. Estimating kinetic parameters from dynamic contrast-enhanced T<sub>1</sub>-weighted MRI of a diffusible tracer: standardized quantities and symbols. *J Magn Reson Imaging* 1999;10:223–232.
- Gallez B, Jordan BF, Baudelet C, Misson PD. Pharmacological modifications of the partial pressure of oxygen in murine tumors: evaluation using in vivo EPR oximetry. *Magn Reson Med* 1999;42:627–630.
- Snyder SA, Lanzen JL, Braun RD, Rosner G, Secomb TW, Biaglow J, Brizel DM, Dewhirst MW. Simultaneous administration of glucose and hyperoxic gas achieves greater improvement in tumor oxygenation than hyperoxic gas alone. *Int J Radiat Oncol Biol Physiol* 2001;51:494–506.
- Burd R, Lavorgna SN, Daskalakis C, Wachsberger PR, Wahl ML, Biaglow JE, Stevens CW, Leeper DB. Tumor oxygenation and acidification are increased in melanoma xenografts after exposure to hyperglycemia and meta-iodo-benzylguanidine. *Radiat Res* 2003;159:328–335.
- Al Hallaq HA, Fan X, Zamora M, River JN, Moulder JE, Karczmar GS. Spectrally inhomogeneous BOLD contrast changes detected in rodent tumors with high spectral and spatial resolution MRI. *NMR Biomed* 2002;15:28–36.